nature medicine

MDM4 is a key therapeutic target in cutaneous melanoma

Agnieszka Gembarska[1,2], Flavie Luciani[1,2], Clare Fedele[3,4], Elisabeth A Russell[5], Michael Dewaele[1,2], Stéphanie Villar[6], Aleksandra Zwolinska[1,2], Sue Haupt[7,8], Job de Lange[9], Dana Yip[10], James Goydos[10], Jody J Haigh[11,12], Ygal Haupt[7,8,13], Lionel Larue[14], Aart Jochemsen[9], Hubing Shi[15,16], Gatien Moriceau[15,16], Roger S Lo[15,16], Ghanem Ghanem[17], Mark Shackleton[3,4,7], Federico Bernal[5] & Jean-Christophe Marine[1,2]

The inactivation of the p53 tumor suppressor pathway, which often occurs through mutations in *TP53* (encoding tumor protein 53) is a common step in human cancer. However, in melanoma—a highly chemotherapy-resistant disease—*TP53* mutations are rare, raising the possibility that this cancer uses alternative ways to overcome p53-mediated tumor suppression. Here we show that Mdm4 p53 binding protein homolog (MDM4), a negative regulator of p53, is upregulated in a substantial proportion (~65%) of stage I–IV human melanomas and that melanocyte-specific Mdm4 overexpression enhanced tumorigenesis in a mouse model of melanoma induced by the oncogene *Nras*. MDM4 promotes the survival of human metastatic melanoma by antagonizing p53 proapoptotic function. Notably, inhibition of the MDM4-p53 interaction restored p53 function in melanoma cells, resulting in increased sensitivity to cytotoxic chemotherapy and to inhibitors of the *BRAF* (V600E) oncogene. Our results identify MDM4 as a key determinant of impaired p53 function in human melanoma and designate MDM4 as a promising target for antimelanoma combination therapy.

Cutaneous melanoma is the leading cause of skin cancer–related deaths and is notorious for its resistance to therapy. Nevertheless, recent targeted therapy trials have been promising[1,2]. Notably, the Ras/Raf/MEK/ERK pathway has been identified as a major, druggable regulator of melanoma[3]. Activating *NRAS* mutations are commonly observed in human melanoma, usually affecting codon 61 (refs. 4,5). *BRAF* is also frequently mutated[6], most commonly resulting in a glutamic acid for valine substitution at position 600 (V600E) (ref. 6).

BRAF (V600E), which results in constitutively overactive MAPK/ERK signaling and melanocyte hyperproliferation[7], has been successfully exploited for targeted therapy. PLX4032 (vemurafenib), a selective RAF inhibitor, showed an unprecedented antitumor response rate in patients with *BRAF* (V600E) (ref. 8) and conferred an overall survival benefit in a pivotal phase 3 study[9]. Unfortunately, most patients rapidly acquire resistance to vemurafenib[10], highlighting the urgent need for new treatment strategies of *BRAF* (V600E)-induced melanoma.

Restoration of the wild-type p53 tumor suppressor function has emerged as an attractive anticancer strategy[11–13]. However, usefulness of this approach in melanoma is unclear; although inactivating mutations or allelic loss of *TP53* are common in human cancers[14], the *TP53* locus is intact in >95% of melanomas[15]. Nevertheless, increasing evidence supports a role for p53 in melanomagenesis, as loss of p53 cooperates with activated $HRAS^{V12G}$ and $BRAF^{V600E}$ in mice[16,17] and with oncogenic NRAS in zebrafish[18], culminating in melanoma formation.

Cancers that retain wild-type p53 often find alternative ways to subvert p53 function, by deregulating upstream modulators and/or by inactivating downstream effectors[19]. For example, *MDM2*, which encodes an E3 ubiquitin ligase that controls p53 expression and function[20], is amplified in 3–5% of human melanomas[21].

Here we show that the p53 pathway is inactivated in the majority of cutaneous melanomas as a result of upregulated expression of MDM4, a key negative regulator of p53 (refs. 22,23). We show that targeting the MDM4-p53 interaction inhibits the growth of melanoma cells and markedly sensitizes them to conventional chemotherapeutics. Notably, MDM4 inhibition affects the growth of melanoma cells that have acquired resistance to BRAF inhibitors and synergizes with BRAF

[1]Center for the Biology of Disease, Laboratory for Molecular Cancer Biology, Vlaams Instituut voor Biotechnologie (VIB), Leuven, Belgium. [2]Center for Human Genetics, Katholieke Universiteit (KU) Leuven, Leuven, Belgium. [3]Melanoma Research Laboratory, Peter MacCallum Cancer Centre, East Melbourne, Australia. [4]Department of Pathology, The University of Melbourne, Parkville, Australia. [5]Metabolism Branch, Center for Cancer Research, National Cancer Institute, US National Institutes of Health, Bethesda, Maryland, USA. [6]International Agency for Research on Cancer (IARC/CIRC), Lyon, France. [7]Sir Peter MacCallum Department of Oncology, The University of Melbourne, Parkville, Australia. [8]Peter MacCallum Cancer Centre, Research Division, East Melbourne, Australia. [9]Department of Molecular Cell Biology, University Medical Centre, Leiden, The Netherlands. [10]Robert Wood Johnson Medical School, University of Medicine and Dentistry of New Jersey, Cancer Institute of New Jersey, New Brunswick, New Jersey, USA. [11]Vascular Cell Biology Unit, Department for Molecular Biomedical Research, VIB, Ghent, Belgium. [12]Department of Biomedical Molecular Biology, Ghent University, Ghent, Belgium. [13]Department of Biochemistry and Molecular Biology, Monash University, Melbourne, Australia. [14]Curie Institute, Developmental Genetics of Melanocytes, Centre National de la Recherche Scientifique (CNRS) UMR3347, Institut National de la Santé et de la Recherche Médicale (INSERM) U1021, Orsay, France. [15]Department of Medicine (Division of Dermatology, Jonsson Comprehensive Cancer Center, David Geffen School of Medicine, University of California Los Angeles, Los Angeles, California, USA. [16]Department of Molecular and Medical Pharmacology, Jonsson Comprehensive Cancer Center, David Geffen School of Medicine, University of California Los Angeles, Los Angeles, California, USA. [17]Institute Jules Bordet, Brussels, Belgium. Correspondence should be addressed to J.-C.M. (jeanchristophe.marine@cme.vib-kuleuven.be).

Received 14 November 2011; accepted 13 June 2012; published online 22 July 2012; doi:10.1038/nm.2863

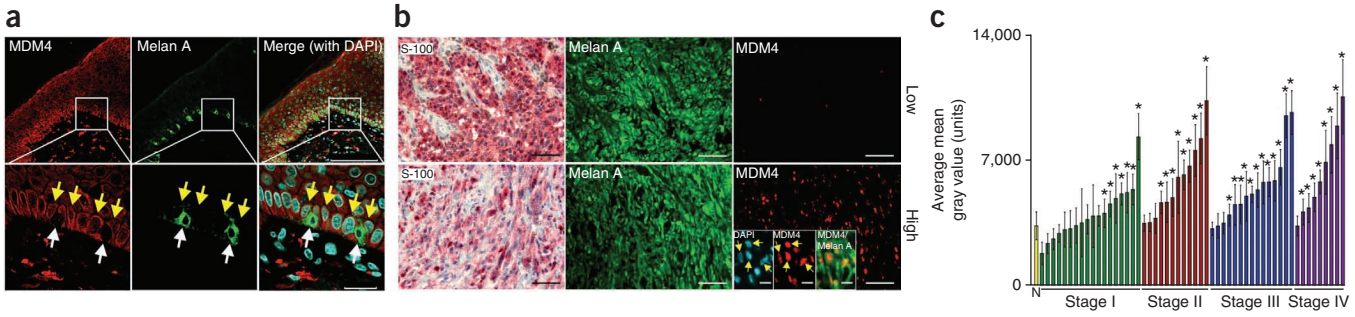

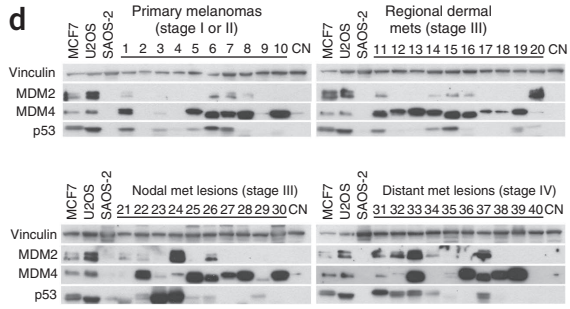

Figure 1 MDM4 is frequently overexpressed in human melanoma. (**a**) Immunofluorescence images of normal human skin co-stained for MDM4 (red) and the melanocyte marker Melan A (green). Nuclei are stained with DAPI (blue). High magnification images show that MDM4 was detected in the cytoplasm of keratinocytes (yellow arrows), but was very low to undetectable in normal melanocytes (white arrows). Scale bar, 25 μm. (**b**) Representative immunofluorescence staining of human melanomas showing low (top) and high (bottom) MDM4 expression. We confirmed melanoma status by Melan A (green) in the same section and S-100 in adjacent sections. Inset images in MDM4-high tumor show nuclear localization of MDM4 (yellow arrows) as determined by DAPI staining of the same section. Scale bars, 50 μm (10 μm in insets). (**c**) MDM4 protein expression, determined by immunofluorescence, in 54 human melanomas from clinical disease stages I–IV. Graphs represent the average MDM4 mean gray value (MGV) ± s.d. of at least 50 cells per sample. Asterisks show significantly increased MDM4 MGV compared to normal (N) melanocytes (*$P < 0.01$). (**d**) Immunoblotting analysis of expression levels of MDM2, MDM4 and p53 protein in human melanoma samples, in cancer cell lines and in congenital melanocytic nevi (CN). The samples are arranged into four clinically distinct subtypes: (primary cutaneous melanomas, regional dermal metastases, nodal metastases and distant metastases). MCF7, U2OS and SAOS-2 cells are reference controls and vinculin-specific immunoblotting is used to detect differences in sample loading.

inhibitors to kill BRAF-mutant cells. These data identify the MDM4-p53 interaction as a new therapeutic target for melanoma treatment.

RESULTS

MDM4 is overexpressed in ~65% of human melanomas

To investigate whether MDM4 overexpression contributes to p53 inactivation in human melanomas, we assessed MDM4 protein expression in normal skin and in melanomas by immunofluorescence. Although detectable in the cytoplasm of epidermal keratinocytes, MDM4 expression was very low to undetectable in normal melanocytes (**Fig. 1a**). Assessment of a panel of 54 primary cutaneous and metastatic melanomas showed variable MDM4 expression (from very low or undetectable to high), with MDM4 localizing to the nucleus in most cells (**Fig. 1b**). We observed that MDM4 expression was significantly increased in 68.5% of melanomas compared with normal melanocytes (**Fig. 1c**), including 56.7% of early stage (stage I or II) tumors and 83.3% of metastatic (stage III or IV) tumors (**Fig. 1c**). We found no correlation between age (calculated as age at resection of tumor) or pathologic subtype and MDM4 expression (**Supplementary Table 1**). There was, however, a statistically significant correlation between high MDM4 expression and late-stage (stage III or IV) metastatic disease (**Supplementary Table 1**).

We confirmed MDM4 overexpression in an additional cohort of 40 freshly isolated human melanomas by immunoblotting (**Fig. 1d**). Notably, in only 3 out of 40 of these samples were *MDM4* mRNA levels comparable to or higher than those in the breast cancer cell line MCF-7, which is known to express high *MDM4* mRNA levels (**Supplementary Fig. 1**)[24]. In contrast, MDM4 protein expression was comparable to or higher than that observed in MCF-7 cells in 65% of cases (**Fig. 1d** and **Supplementary Table 2**). Consistent with the immunofluorescence data, MDM4 protein expression was either undetectable or very low in normal melanocytes and in benign nevi (**Fig. 1d** and **Supplementary Fig. 2a**). Six out of ten primary cutaneous tumors had high MDM4 levels (**Fig. 1d**), supporting the possibility that MDM4 upregulation occurs early in melanomagenesis. In contrast, MDM2 protein expression levels ranged from undetectable to low in most cases (**Fig. 1d**). We only found MDM2 expression levels comparable to those in U2OS cells, an osteosarcoma cell line highly expressing MDM2, in one out of ten regional dermal metastases, one out of ten nodal metastases and four out of ten distant metastases (**Fig. 1d** and **Supplementary Table 1**). Overexpression of MDM2 and MDM4 co-occurred in only 2 out of 30 metastatic melanomas (stage IV) (**Fig. 1d**).

Compared with primary melanocytes, we found that MDM4 was also elevated in 14 out of 16 patient-derived short-term cultures established from metastatic tumors, as well as in four out of four cell lines (A375, WM9, Mel-501, Lu1205) harboring wild-type p53 (**Supplementary Fig. 2b**,**c** and **Supplementary Table 3**). Consistent with the notion of a post-transcriptional mechanism being primarily responsible for MDM4 upregulation, *MDM4* mRNA levels were higher than those in MCF-7 in only one of these cell lines (MM120; **Supplementary Fig. 1b**). As in freshly isolated human melanoma samples, MDM2 protein expression levels ranged from undetectable to low in the majority of short-term cultures (**Supplementary Fig. 2b**,**c**). We found that MDM2 levels were comparable to those in U2OS cells in four cell lines (MM011, MM034, MM061, MM117) and higher in only two cell lines (MM001, MM120; **Supplementary Table 3**). Notably, MDM2 was highly expressed in all (four out of four) well-established (**Supplementary Fig. 2c**) melanoma cell lines, suggesting that extended *in vitro* passage might induce MDM2 expression.

We determined *TP53*, *BRAF* and *NRAS* mutational status in the primary tumors and cell lines described above (**Supplementary Tables 2** and **3**). Consistent with previous reports[15,25], *TP53* mutations

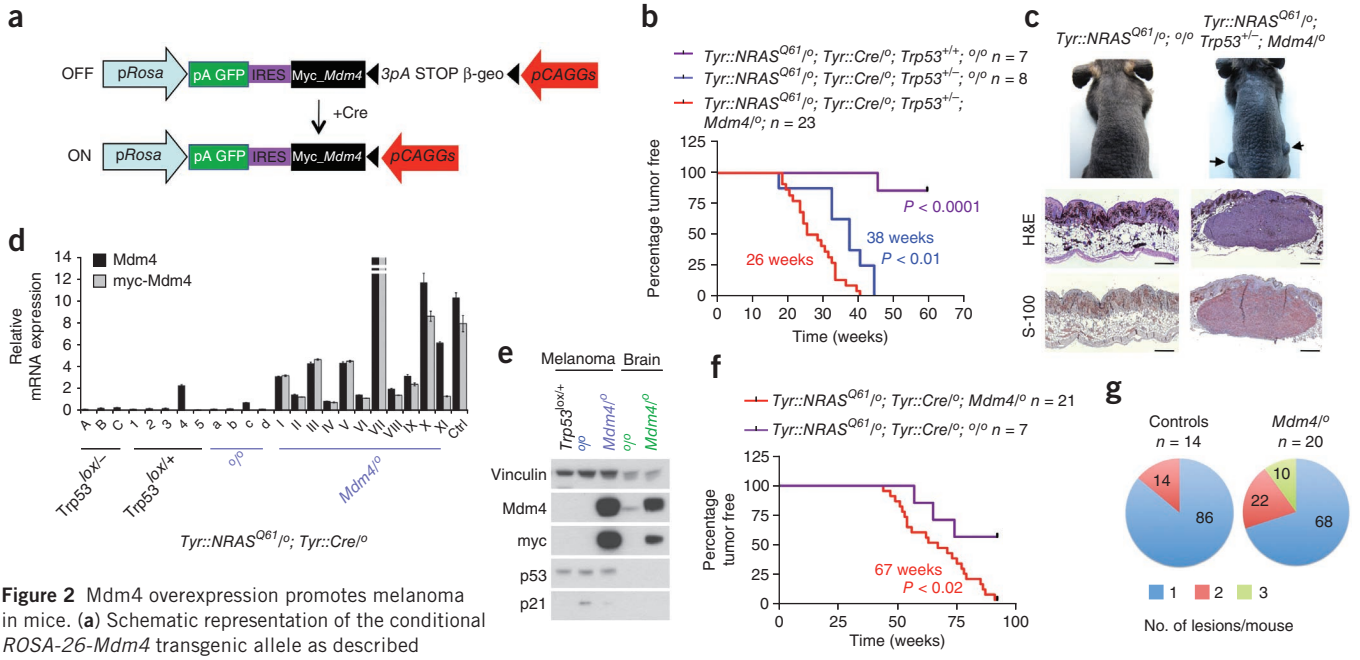

Figure 2 Mdm4 overexpression promotes melanoma in mice. (**a**) Schematic representation of the conditional *ROSA-26-Mdm4* transgenic allele as described previously[30]. A single copy of the *Mdm4* transgene is inserted into the *ROSA26* locus by homologous recombination. Before Cre-mediated excision the *pCAGG* promoter drives the expression of the β-geo STOP cassette only. Upon Cre expression the floxed β-geo STOP cassette is excised and Myc-*Mdm4*-IRES-eGFP is transcribed. (**b**) Penetrance of malignant melanoma upon melanocyte-specific Mdm4 overexpression. Kaplan-Meier curves showing increased melanoma incidence in *Tyr::NRAS^{Q61}/o; Tyr::Cre/o; Trp53$^{+/-}$; Mdm4/o* mice by comparison with the group of controls (*Tyr::NRAS^{Q61}/o; Tyr::Cre/o; Trp53$^{+/-}$; o/o* and *Tyr::NRAS^{Q61}/o; Tyr::Cre/o; Trp53$^{+/+}$; o/o*). (**c**) External views and H&E staining (middle) and immunohistochemistry (IHC) for S-100 (bottom) in the skin of mice with the indicated genotypes. Scale bars, 500 μm. (**d**) Reverse-transcription quantitative PCR (RT-qPCR) analysis of Mdm4 expression in tumor samples derived from mice with the indicated genotypes (samples A–C from *Tyr::NRAS^{Q61}/o; Tyr::Cre/o; Trp53$^{lox/-}$*; samples 1–5 from *Tyr::NRAS^{Q61}/o; Tyr::Cre/o; Trp53$^{lox/+}$*; samples a–d from *Tyr::NRAS^{Q61}/o; Tyr::Cre/o; Trp53$^{+/-}$; o/o*; samples I–XI from *Tyr::NRAS^{Q61}/o; Tyr::Cre/o; Trp53$^{+/-}$; Mdm4/o*). One primer pair allows specific detection of Myc-tagged exogenous Mdm4 (myc-Mdm4; gray bars) and the other pair detects both endogenous and exogenous Mdm4 expression (black bars). Elevated Mdm4 expression is observed at the transcriptional level in samples from *Tyr::NRAS^{Q61}/o; Tyr::Cre/o; Trp53$^{+/-}$; Mdm4/o* mice. The data represent the means ± s.d. of three technical replicates. (**e**) Western blot analysis confirming high Myc-tagged exogenous Mdm4 expression in a *Tyr::NRAS^{Q61}/o; Tyr::Cre/o; Trp53$^{+/-}$; Mdm4/o* (blue *Mdm4/o*) melanoma lesion and not in lesions from *Tyr::NRAS^{Q61}/o; Tyr::Cre/o; Trp53$^{+/-}$; o/o* (blue *o/o*) or *Tyr::NRAS^{Q61}/o; Tyr::Cre/o; Trp53$^{lox/+}$* (*Trp53$^{lox/+}$*). As previously described[30], high expression levels of Mdm4 are seen in the brain of *Sox2Cre/o; Mdm4/o* mice (green *Mdm4/o*). Endogenous Mdm4 expression is also detected in the brain of *Sox2Cre/o; o/o* mice (green *o/o*). p53 and p21 protein levels were also examined in these samples. Vinculin serves as a loading control. (**f**) Penetrance of malignant melanoma upon melanocyte-specific overexpression of Mdm4 on a *Trp53* wild-type background. Kaplan-Meier curves showing increased melanoma incidence in *Tyr::NRAS^{Q61}/o; Tyr::Cre/o; Mdm4/o* mice in comparison with the control group (*Tyr::NRAS^{Q61}/o; Tyr::Cre/o; o/o*) ($P = 0.0156$). (**g**) Percentage of the number of melanoma lesions per mouse in *Tyr::NRAS^{Q61}/o; Tyr::Cre/o; Mdm4/o* (*Mdm4/o* mice) and in the control groups (*Tyr::NRAS^{Q61}/o; Tyr::Cre/o; o/o* and *Tyr::NRAS^{Q61}/o; o/o; Mdm4/o*). These percentages differed significantly between the two cohorts ($P < 0.05$).

were rare (**Supplementary Tables 2** and **3**). Notably, we found that MDM4 was overexpressed at comparable frequencies in tumors and cell lines harboring either wild-type or mutated *NRAS* or *BRAF* (**Supplementary Tables 2** and **3**).

MDM4 promotes melanoma in mice

Constitutive expression of an activated form of human NRAS (NRAS^{Q61K}) in melanocytes leads to formation of aggressive melanomas in *Tyr::NRAS^{Q61}/o* transgenic mice (mice that carry one copy of the *NRAS^{Q61K}* transgene)[26]; however, melanomas develop only after a long latency and with low penetrance. To assess the role of p53 in these mice, we inactivated *Trp53* in previously characterized null (–) and conditional (*lox*) knockout alleles[27,28]. Melanocyte-specific deletion of one or two alleles of *Trp53* cooperated with NRAS^{Q61K} to induce spontaneous and aggressive melanoma formation (ref. 29 and **Supplementary Fig. 3**). Although indicative of p53's role as a barrier to melanomagenesis *in vivo*, these experiments do not recapitulate the genetic makeup of human melanomas, most of which express wild-type p53 (ref. 15).

We reasoned that MDM4 could compromise p53 function *in vivo* to promote melanoma formation. We therefore induced Mdm4 overexpression in melanocytes of *Tyr::NRAS^{Q61}/o* and *Tyr::Cre/o; Trp53$^{lox/-}$* mice by crossing these mice with the previously described Mdm4 conditional transgenic mice *ROSA26-pCAGGs-(loxP-STOP-loxP)-Mdm4/o* (mice carrying one copy of an Mdm4 conditional transgenic allele, referred to as *Mdm4/o*)[30] (**Fig. 2a**). We crossed these double-transgenic mice onto a *Trp53*-heterozygous background to facilitate spontaneous tumor development. As expected from the *Trp53* heterozygosity of *Tyr::NRAS^{Q61}/o; Tyr::Cre/o; Trp53$^{+/-}$; Mdm4/o* mice, some mice developed T cell lymphomas and sarcomas[27] (data not shown). However, the vast majority of mice developed melanoma before developing other tumors (data not shown). We restricted further analyses to mice that were lymphoma- and sarcoma-free and that developed melanomas at least 3-mm thick. Quadruple-transgenic mice (*Tyr::NRAS^{Q61}/o; Tyr::Cre/o; Trp53$^{+/-}$; Mdm4/o*) developed at least one melanoma significantly faster than controls (*Tyr::NRAS^{Q61}/o; Tyr::Cre/o; Trp53$^{+/-}$; o/o*) (**Fig. 2b**). Melanomas were nodular, pigmented and

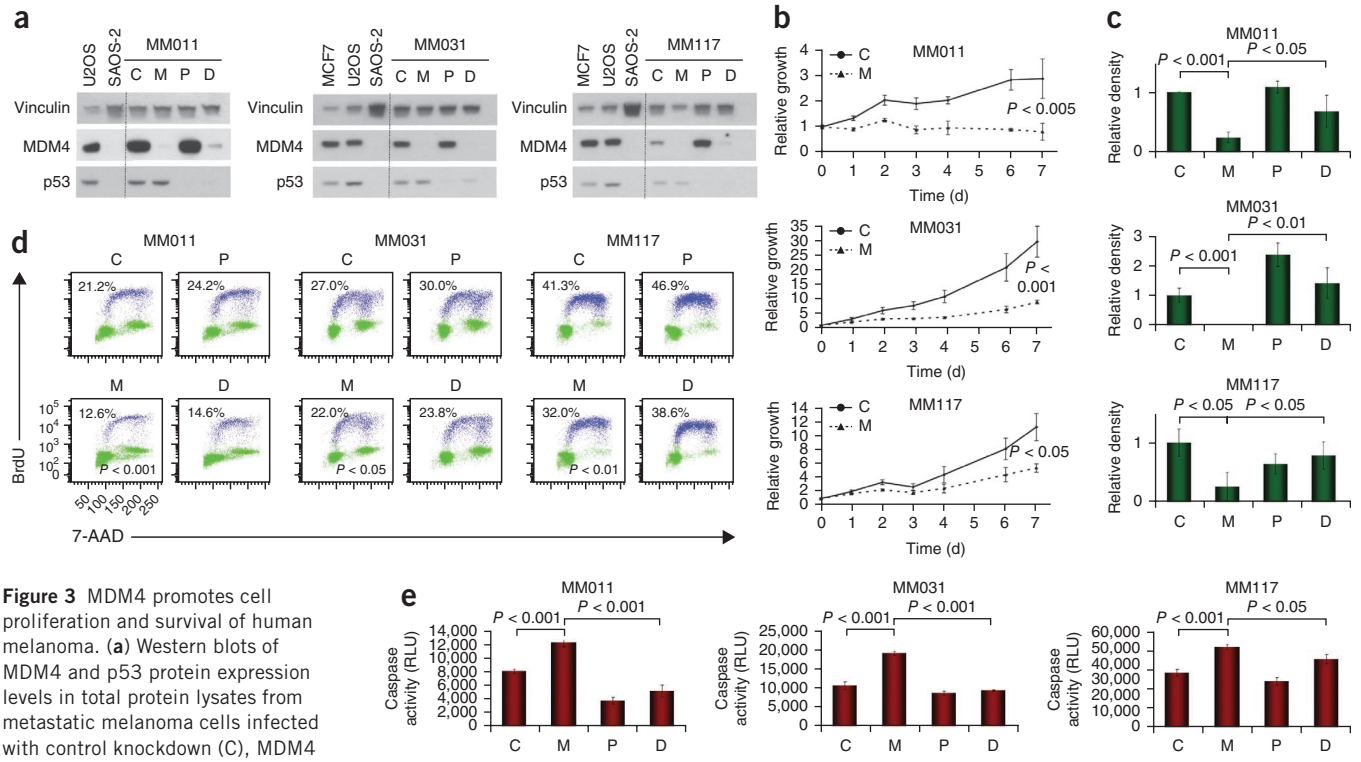

Figure 3 MDM4 promotes cell proliferation and survival of human melanoma. (**a**) Western blots of MDM4 and p53 protein expression levels in total protein lysates from metastatic melanoma cells infected with control knockdown (C), MDM4 knockdown (M), p53 knockdown (P), and both MDM4 knockdown and p53 knockdown (D) vectors, as well as in the MCF-7, U2OS and SAOS-2 reference cell lines. The lines separate lanes that were not consecutive on the original western blot. (**b**) WST-1 assay of cell growth of the infected metastatic melanoma cells. Data represent the mean of three biological replicates. (**c**) Low-density colony formation assays 12 d after seeding, showing cell growth of the infected metastatic melanoma cells. The data are presented as the mean density of three different biological replicates ± s.d. (**d**) Fluorescence-activated cell sorting (FACS) analysis (dot plot) showing the percentage of BrdU-positive cells for one typical experiment in control knockdown (C), MDM4 knockdown (M), p53 knockdown (P) and MDM4/p53 double–knockdown (D) cultures. Data are from three independent infection experiments; C and M are significantly different (*P* values are indicated in the M dot plots). 7-AAD, 7-aminoactinomycin D. (**e**) Caspase3/7-Glo luminescence assays done in C, M, P and D cultures. The data are presented as the means of three different biological replicates ± s.d.; C and M and M and D are significantly different in all cell lines (*P* values are indicated on the graphs).

positive for S-100 protein expression[31], regardless of genotype (**Fig. 2c**). Tumors arising in *Tyr::NRAS*$^{Q61/o}$*; Tyr::Cre/*^{o}*; Mdm4/*^{o} mice retained high exogenous (myc-tagged) Mdm4 expression (**Fig. 2d,e**). Exogenous Mdm4 mRNA and protein expression levels were perfectly correlated.

We next assessed whether Mdm4 overexpression also enhances melanoma development on a wild-type *Trp53* background. *Tyr::NRAS*$^{Q61/o}$*; Tyr::Cre/*^{o}*; Mdm4/*^{o} had a nearly 100% incidence of melanoma with a much shorter average latency period than controls (*Tyr::NRAS*$^{Q61/o}$*; Tyr::Cre/*^{o}*;* $^{o/o}$) (**Fig. 2f**). On average, there were more lesions per mouse in Mdm4-overexpressing mice than in controls (**Fig. 2g**). Together, these data indicate that Mdm4 overexpression cooperates with the NRAS oncoprotein to promote aggressive melanoma formation *in vivo*.

MDM4 promotes cell proliferation and survival of human melanoma

To test whether human metastatic melanoma cells depend on high MDM4 expression for their survival and proliferation we knocked down *MDM4* in short-term cultured (MM011, MM031, MM117) and commonly used metastatic melanoma cell lines (A375, Lu1205). Our choice of cell lines was motivated by the presence of high protein expression levels of MDM4, a genetically intact *TP53* pathway and different ratios of MDM4/MDM2 protein expression levels. We targeted different regions of MDM4 mRNA using two lentiviral constructs (data shown below and in **Supplementary Fig. 4**). MM031 expressed high MDM4 and low MDM2 protein expression levels, which best represents the vast majority of melanoma lesions; MM011 and MM117 highly express both MDM4 and MDM2, which is characteristic of only a few human distant-metastatic melanomas. Western blotting confirmed efficient MDM4 knockdown in all cell lines (**Fig. 3a** and **Supplementary Fig. 5a**). Cell viability and colony formation assays showed that MDM4 knockdown caused robust growth inhibition in all melanoma lines analyzed (**Fig. 3b,c** and **Supplementary Fig. 5b,c**).

Cell cycle analysis showed a reproducible and significant decrease in BrdU incorporation upon MDM4 knockdown (**Fig. 3d** and **Supplementary Fig. 5d**). In addition to the reduced proliferation, increased cell death was evidenced by the increased sub-G1 fraction in the FACS profiles (data not shown). We found that cell death resulted, at least in part, from a reproducible and significant induction of caspase3/7 activity (**Fig. 3e** and **Supplementary Fig. 5**).

Some of the parental melanoma cell lines (MM031, Lu1205, A375) efficiently formed tumors when injected into nude mice (8-week-old Rj:NMRI-nu (nu/nu) female mice). We show that MDM4 knockdown strongly reduces the transforming potential of these cells *in vivo* (**Supplementary Figs. 5f** and **6**). These data indicate that MDM4 regulates the survival and proliferation of high-MDM4-expressing melanoma cells *in vitro* and *in vivo*.

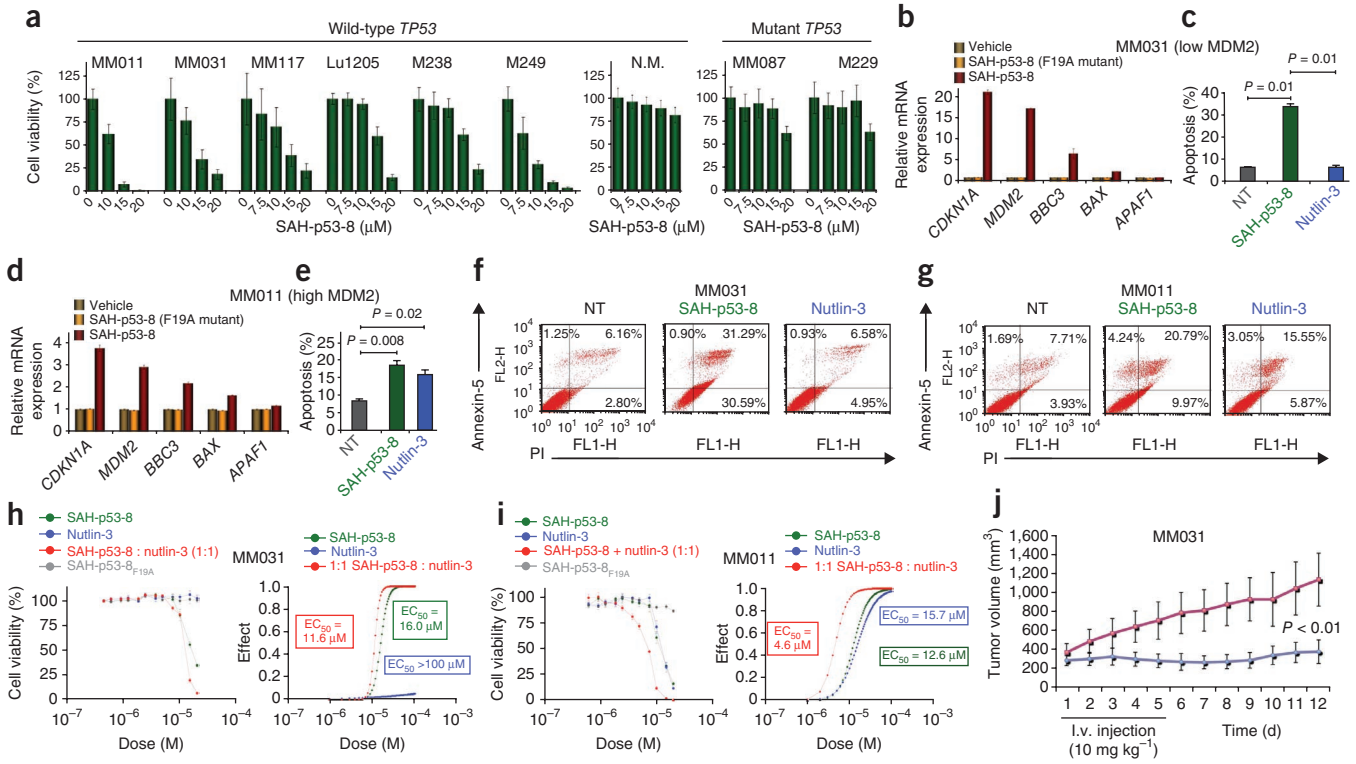

Figure 4 Inhibition of the MDM4-p53 interaction restores p53 activity in melanoma. (**a**) Cell viability of normal human melanocytes (N.M.) and melanoma cells harboring wild-type or mutant *TP53* treated with increasing dose of SAH-p53-8 for 24 h. Data represent the mean ± s.d. of three biological replicates. (**b**–**g**) RT-qPCR mRNA expression analysis and Annexin V apoptosis assay. (**b**,**d**) mRNA expression of selected p53 target genes (*CDKN1A*, *MDM2*, *BBC3*, *BAX*, *APAF1*) in the MM031 (**b**) and MM011 (**d**) melanoma cell lines 24 h after SAH-p53-8 treatment (EC_{50} of SAH-p53-8 used per each cell line); SAH-p53-8_{F19A} is used as a point mutant control and dimethyl sulfoxide (DMSO) as a vehicle control. The data are the means ± s.d. from three technical replicates. The values are normalized to the levels of mRNA expression in vehicle-treated cells (set to 1). (**c**,**e**–**g**) Annexin V apoptosis assay on MM031 and MM011 melanoma cells treated with vehicle, EC_{50} of SAH-p53-8 (16 μM for MM031 and 10 μM for MM011) or equivalent dose of nutlin-3 for 24 h. We incubated cells with Alexa Fluor 488–conjugated annexin V and propidium iodide (PI). (**c**,**e**) Mean percentage ± s.d. of apoptotic cells from three independent biological replicates; whereas we found that SAH-p53-8 ($P = 0.01$) but not nutlin-3 induced a significant apoptotic response in the MM031, MM011 responded to both agents ($P = 0.008$ and $P = 0.02$ for SAH-p53-8 and nutlin-3, respectively). (**f**,**g**) FACS data from a representative experiment are shown. Values represent the percentage of cells that are positive for either Annexin-5 or PI. (**h**,**i**) Viability of MM031 (**h**, left) and MM011 (**i**, left) melanoma cell lines treated with 0.5–20 μM SAH-p53-8, nutlin-3, or an equimolar combination for 24 h. Data are means ± s.d. for experiments done in at least triplicate. Dose-effect synergy analyses of MM031 (**h**, right) and MM011 (**i**, right) melanoma cells treated with 0.5–20 μM SAH-p53-8, nutlin-3, or an equimolar combination. The EC_{50} values for each treatment are indicated. (**j**) SAH-p53-8 overcomes MDM4-mediated p53 suppression and blocks tumor growth *in vivo*. Tumor volume of cohorts of MM031 xenograft mice treated with vehicle (5% (vol/vol) DMSO in D5W) or 10 mg kg^{-1} SAH-p53-8 by i.v. injection daily for 5 consecutive days. Data are means ± s.d. of seven different biological replicates ($P < 0.01$ on day 12). Bottom, external views of representative tumor-bearing mice on day 12. Scale bar, 1.5 cm.

MDM4 protects melanoma against p53-induced apoptosis

To test whether p53 inactivation underlies dependency of melanoma on high MDM4 expression, we knocked down both MDM4 and p53 in short-term cultured metastatic melanoma cell lines (MM011, MM031, MM117; **Fig. 3a**). Colony formation assays indicated that the MDM4 KD-mediated growth inhibition at least partly depends on p53 (**Fig. 3c**).

The two best-characterized p53-mediated antigrowth activities are induction of cell cycle arrest and apoptosis. Unexpectedly, p53 knockdown did not significantly rescue the proliferation of melanoma cells upon MDM4 knockdown (**Fig. 3d**). In contrast, p53 knockdown largely rescued MDM4 knockdown cells from apoptosis (**Fig. 3e**). Concomitant with apoptosis induction upon MDM4 knockdown, we observed increased recruitment of p53 to the promoters of its proapoptotic targets, *BAX* (encoding BCL2-associated X protein) and *APAF1* (encoding apoptotic peptidase activating factor 1), and a marked increase in their transcription (**Supplementary Fig. 7**). The data suggest that high MDM4 levels inhibit apoptosis in human melanoma cells by antagonizing p53.

Inhibition of the MDM4-p53 interaction restores p53 activity

The reliance of melanoma cells on MDM4 for survival suggests that interfering with its interaction with p53 could restore apoptotic capability. SAH-p53-8 is a cell-penetrating, stabilized, α-helical peptide[32] that binds with high affinity to MDM4 within its p53-binding pocket and is capable of disrupting p53-MDM4 complexes[33]. SAH-p53-8 has approximately 25-fold lower potency against MDM2 *in vitro*[33]. Unlike the MDM2-specific antagonist nutlin-3 (ref. 34), SAH-p53-8 can reactivate p53 and induce apoptosis in cancer cells that highly express MDM4 and wild-type p53 (ref. 33). To test whether direct

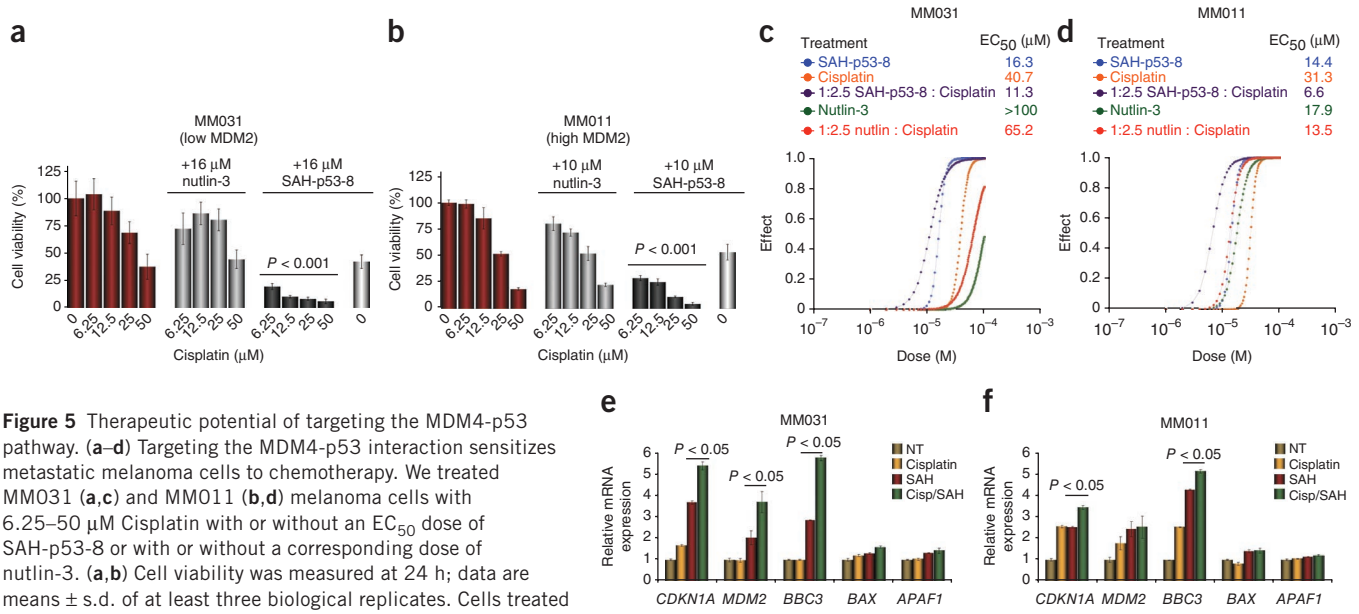

Figure 5 Therapeutic potential of targeting the MDM4-p53 pathway. (**a**–**d**) Targeting the MDM4-p53 interaction sensitizes metastatic melanoma cells to chemotherapy. We treated MM031 (**a**,**c**) and MM011 (**b**,**d**) melanoma cells with 6.25–50 μM Cisplatin with or without an EC_{50} dose of SAH-p53-8 or with or without a corresponding dose of nutlin-3. (**a**,**b**) Cell viability was measured at 24 h; data are means ± s.d. of at least three biological replicates. Cells treated with SAH-p53-8 show a statistically significant decrease in cell viability ($P < 0.001$) compared with cells treated with Cisplatin alone. (**c**,**d**) Dose effect synergy analyses of MM031 (**c**) and MM011 (**d**) melanoma cells treated with 6,25-50 μM Cisplatin with or without 0,5-20 μM SAH-p53-8 or nutlin-3. (**e**,**f**) RT-qPCR mRNA expression analysis of selected p53 target genes in the MM031 (**e**) and MM011 (**f**) melanoma cell lines 24 h after treatment. The data represent the means ± s.d. from three technical replicates. The values are normalized to the level of mRNA expression in vehicle-treated cells (set to 1). *CDKN1A*, *MDM2* and *BBC3* mRNA expression levels differed significantly in cells treated with both Cisplatin and SAH-p53-8 compared with cells treated with the single agents ($P < 0.05$) in both cell lines.

inhibition of MDM4 is a viable therapeutic strategy for melanoma, we treated a series of melanoma cell lines, including the BRAF inhibitor–sensitive melanoma M238, M249 and M229 cell lines[35], with increasing concentrations of SAH-p53-8. SAH-p53-8 potently inhibited growth of all melanoma lines carrying wild-type p53 (**Fig. 4a** and **Supplementary Fig. 8**). In contrast, melanoma cells with inactive p53 mutants did not respond to SAH-p53-8 treatment, indicating that SAH-p53-8-mediated growth inhibition depends on the presence of wild-type p53 (**Fig. 4a**). Moreover, SAH-p53-8 did not markedly affect normal melanocyte growth (**Fig. 4a**). SAH-p53-8, but not its biologically inactive point-mutant analog SAH-$p53\text{-}8_{F19A}$, induces expression of p53-target genes, including *BAX*, *APAF1* and *BBC3* (also known as *PUMA;* encoding BLC2 binding component 3) in both MM031 and MM011 (**Fig. 4**). SAH-p53-8 induced apoptosis in all melanoma cell lines; this effect was significantly attenuated by knockdown or hypomorphic mutation of p53 (**Fig. 4** and **Supplementary Fig. 9**).

Consistent with the fact that high MDM4 expression levels are associated with a reduced apoptotic response to MDM2 antagonists[36,37], nutlin-3 induced relatively low apoptotic activity in MM011 cells despite high expression levels of MDM2 in these cells, and it induced practically no activity in MM031 cells (**Fig. 4e**–**g**).

We next treated melanoma cells with SAH-p53-8, nutlin-3 or a 1:1 stoichiometric combination of both compounds (**Fig. 4h**,**i**). As expected, nutlin-3 had only a marginal cytotoxic effect on MM031 cells. In contrast, we observed marked growth inhibition in MM031 cells in response to SAH-p53-8 alone (**Fig. 4h**), and we saw only a very modest increase in cytotoxicity upon combination with nutlin-3 (combination index = 0.90; combination index is calculated as described in ref. 33). MM011 cells, however, showed sensitivity to the single agents (**Fig. 4i**) and the two compounds synergize strongly, leading to enhanced cytotoxicity (combination index = 0.32). The mutant $SAH\text{-}p53\text{-}8_{F19A}$ peptide did not induce any measurable cytotoxic effects in any of the cell lines (**Fig. 4h**,**i**). Together our data indicate that all human melanoma cell lines analyzed are either highly sensitive to MDM4 inhibition either alone or in combination with MDM2 inhibition.

To test the therapeutic potential of inhibiting the p53-MDM4 interaction *in vivo*, we evaluated the activity of SAH-p53-8 in a MM031 mouse xenograft model. Although tumor growth rate was unaffected in vehicle-treated (vehicle was 5% (vol/vol) DMSO in D5W) mice, intravenous treatment with SAH-p53-8 significantly suppressed tumor growth (**Fig. 4j**). As previously shown, histological examination of SAH-p53-8-treated mice indicated no obvious toxicity[33]. Collectively, these data show the therapeutic potential of inhibiting the MDM4-p53 interaction in melanoma.

SAH-p53-8 sensitizes melanoma to chemotherapy and BRAF (V600E) inhibition

DNA-damaging agents such as Cisplatin or melphalan have yielded low response rates in the treatment of melanomas[38]. As these agents rely partly on activating the p53 pathway, we hypothesized that co-treatment with p53-MDM4 inhibitors may enhance their potency. We therefore investigated the effects of Cisplatin and melphalan alone or in combination with either nutlin-3 or SAH-p53-8 on MM011 and MM031 cell line growth. Although treatment with these agents alone yielded variable growth inhibition, cytotoxic effects were greatly potentiated by co-treatment with SAH-p53-8 (**Fig. 5a**–**d** and **Supplementary Fig. 10**). Transcriptional induction of p53 targets was more robust in cells treated with both Cisplatin and SAH-p53-8 than in cells treated with single agents (**Fig. 5e**,**f**). As expected, MM031 cells expressing low levels of MDM2 responded more favorably to the combination of alkylating agents with SAH-p53-8 than to co-treatment with nutlin-3 (**Fig. 5a**,**c**). In contrast, high expression levels of MDM2 rendered MM011 cells at least partly sensitive to nutlin-3 (**Fig. 5b**,**d**); identical results were obtained with melphalan

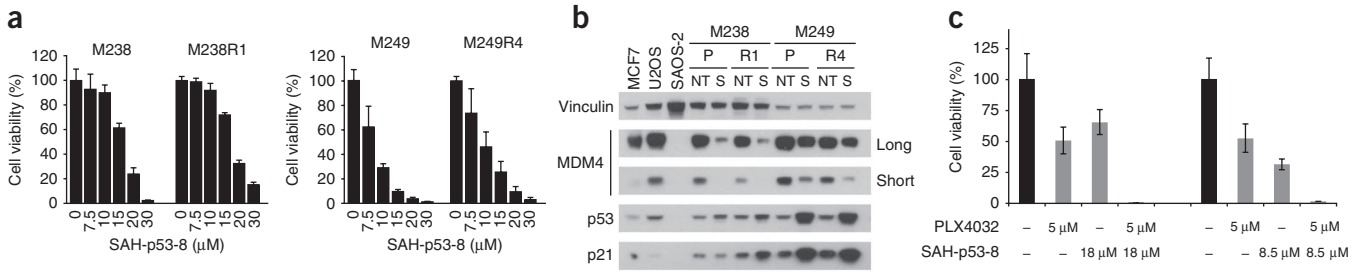

Figure 6 Targeting the MDM4-p53 pathway sensitizes melanoma cells to a $BRAF^{V600E}$-inhibitor. (**a**) We exposed Isogenic BRAF inhibitor–sensitive parental and BRAF inhibitor–resistant cell lines to increasing doses of SAH-p53-8 (7.5–30 μM). We measured cell viability 24 h after SAH-p53-8 treatment. Data represent the means ± s.d. of three biological replicates. (**b**) MDM4, p53 and p21 protein levels assessed by western blotting analysis in nontreated (NT) and SAH-p53-8 (S)-treated human melanoma cells M238, M238R1, M249 and M249R4, which were described previously[35]. We used MCF7, U2OS and SAOS-2 cells as reference controls; vinculin is a loading control. P; parental, R; BRAF inhibitor–resistant subline. Long and Short indicate long and short exposure, respectively. (**c**) Dose-effect synergy analyses of melanoma cells treated with 5 μM PLX4032 and an EC_{50} dose of SAH-p53-8 (18 and 8.5 μM). Data are means ± s.d. of at least three biological replicates. Response to combination treatment differed significantly from the response to single agents ($P < 0.01$) in both cell lines.

(**Supplementary Fig. 10**). Collectively, these data suggest that targeting the MDM4-p53 interaction sensitizes melanoma cells to DNA-damaging agents.

Overcoming widespread resistance to BRAF inhibitors[39] is likely to require targeting of multiple signaling pathways. We investigated whether targeting the MDM4-p53 interaction could affect the growth of BRAF inhibitor–sensitive parental melanoma cell lines (M238 and M249) as well as BRAF-resistant sublines (M238R1 and M249R4) that were artificially derived by chronic exposure to a BRAF inhibitor[35]. All cell lines express high MDM4 protein expression levels and harbor wild-type p53. Treatment of both parental and BRAF-resistant cell lines with increasing doses of SAH-p53-8 led to decreased viability, indicating that cells that have acquired drug resistance to BRAF inhibitor remain largely sensitive to MDM4-p53 targeting (**Fig. 6a**). We saw a comparable increase in expression of p53 and its target p21 in the parental and resistant lines upon SAH-p53-8 exposure (**Fig. 6b**). Notably, SAH-p53-8 exposure led to a marked decrease in MDM4 protein expression levels (**Fig. 6b**).

To investigate whether combined BRAF (V600E) and MDM4 inhibition synergizes to induce cytotoxicity, we treated BRAF inhibitor–sensitive lines with a BRAF inhibitor, PLX4032, and with SAH-p53-8 individually or in combination (**Fig. 6c**). PLX4032 alone was sufficient to decrease the viability of these cells (**Fig. 6c**). Co-treatment with PLX4032 and SAH-p53-8 significantly enhanced the effect when compared with each individual compound (**Fig. 6c**).

DISCUSSION

Unlike in most other tumor types, *TP53* mutations are rare in melanomas, making the relevance of the p53 pathway in melanomagenesis controversial. Given our observation of MDM4 overexpression in about 65% of melanomas, we contend that MDM4 overexpression is an important oncogenic event that alters p53 function in melanoma in a large proportion of patients.

Because MDM4 overexpression is primarily detected at the protein level, its detection inevitably escaped previous investigations that focused on transcriptomic analyses. This raises a possibility that MDM4 overexpression might be an even more frequent oncogenic event than previously anticipated in other tumor types as well[23].

At physiological levels MDM4 serves as a constitutive buffer against untoward p53 activity[23,40,41]; its oncogenic activity results from its ability to attenuate p53 function[23,24]. Consistent with this, we found that most melanoma cells depend on high MDM4 expression to survive by keeping the proapoptotic functions of p53 in check. Furthermore, we found that high MDM4 expression levels are also required, in a p53-independent manner, by melanoma cells for proliferation in culture. This raises the possibility that MDM4 possesses additional oncogenic functions, independent of p53 suppression. Although p53-independent function(s) may contribute to MDM4-mediated oncogenesis, we found that targeting the MDM4-p53 interaction was sufficient to suppress the growth of metastatic melanoma cells with wild-type p53.

Restoration of p53 function has been extensively pursued as a therapeutic approach in cancers in which, as in most melanomas, p53 function is compromised although the *TP53* locus remains intact[42–44]. Several efforts have focused on blocking MDM2 as a strategy to reactivate p53 (refs. 34,45–48), despite several caveats[49]. One major limitation of MDM2-specific therapy is that tumor cells in which MDM4 expression is high but MDM2 is low respond poorly to MDM2 inhibition[13,33]. We found that most human melanoma cell lines express high MDM4 and low MDM2 levels and indeed respond very poorly to treatment with the MDM2-specific antagonist nutlin-3. In contrast, these cells are extremely sensitive to SAH-p53-8, thus indicating that pharmacological disruption of the MDM4-p53 interaction is required to induce p53 signaling in these cells. Note, however, that SAH-p53-8 can also suppress MDM2-p53 binding to some extent. It therefore cannot be ruled out that SAH-p53-8 effectiveness against melanoma cells with a high MDM4/MDM2 ratio depends, at least partly, on MDM2 targeting. Melanomas that express high levels of both MDM4 and MDM2 are rare, although we found that cell lines with this profile were sensitive to either SAH-p53-8 or nutlin-3 but even more sensitive to combination treatment. Therefore, whereas the majority of melanoma patients may respond poorly to single MDM2 inhibitors, they could benefit greatly from treatment with single MDM4 or dual MDM4/MDM2 antagonists.

Recent data argue that MDM4 inhibition is a more feasible and less hazardous strategy than MDM2 inhibition for restoring p53 function. For instance, genetic ablation of *Mdm2* in normal adult tissues, including those that are quiescent and fully differentiated, leads to pathologies because of the induction of p53-dependent cell death[20]. Hence, toxicity after systemic exposure to potent MDM2 inhibitors is a serious concern. In contrast, ablation of *Mdm4* in most adult somatic tissues leads to either modest or no phenotypic consequences[40,41].

Most patients with metastatic melanoma do not respond to conventional chemotherapy regimens[50]. Our results show that inhibition of

the MDM4-p53 interaction greatly potentiates the cytotoxic effects of two widely used chemotherapeutic agents. MDM4 inhibitors could therefore be used to enhance the effectiveness of conventional therapeutic agents in the treatment of melanoma.

Similarly, despite the initial success with BRAF inhibitors, chronic treatment is invariably associated with the development of drug resistance[39]. Management of BRAF inhibitor resistance is likely to be achieved through combination therapy that targets multiple pathways. We have shown that MDM4 is overexpressed in melanomas harboring mutations in BRAF and NRAS alike, that MDM4-p53 inhibition equally affects the growth of NRAS- and BRAF-mutant melanoma cells and, notably, that MDM4-p53 inhibition is equally effective at inhibiting growth of BRAF-mutant cells before or after they acquire resistance to BRAF inhibitors. We also show that combined treatment with MDM4-p53 inhibitors and BRAF inhibitors synergizes to kill melanoma cells that are sensitive to BRAF inhibition.

Our findings suggest that MDM4-p53 targeting offers a promising approach to improve the clinical benefits of BRAF inhibition. Crucially, our *in vitro* results predict that MDM4-p53 targeted therapy may be effective in cases when BRAF inhibitor resistance has already been acquired and in melanomas with NRAS mutations, for which no specific inhibitors exist. Prioritization should therefore be given to the preclinical development of strategies that inhibit MDM4-mediated suppression of p53 function in human melanoma.

METHODS

Methods and any associated references are available in the online version of the paper.

Note: Supplementary information is available in the online version of the paper.

ACKNOWLEDGMENTS

We thank O.Van Goethem for excellent technical assistance. We thank P. Agostinis, P. Wolter and M. Skipper for helpful discussions and comments on the manuscript. We thank M. Cario-Andre and A. Taïed for materials from human nevi. A. Zwolinska is a recipient of a 'Het Fonds Wetenschappelijk Onderzoek-Vlaanderen (FWO)' scholarship. C. Fedele was supported by a Clare Oliver Memorial Fellowship from the Victorian Cancer Agency. M. Shackleton was supported by fellowships from Pfizer Australia and the Victorian Endowment for Science, Knowledge and Innovation (VESKI). Y. and S. Haupt were supported by the Australian National Health and Medical Research Council (nos. 509197, 1026990 and 628426) and VESKI. R.S. Lo was supported by Stand Up to Cancer, the Joint Center for Translational Medicine, the Eli and Edythe Broad Center of Regenerative Medicine and Stem Cell Research, and the Seaver Institute. This work was supported by the Intramural Research Program of the US National Institutes of Health and the National Cancer Institute, the Association for International Cancer Research (AICR), the Melbourne Melanoma Project, the Victorian Cancer Agency and the 'Belgian Foundation against Cancer'.

AUTHOR CONTRIBUTIONS

A.G. did experimental work, developed the hypothesis, analyzed the data and coordinated the project. F.L. did experimental work and analyzed the data. C.F. conducted immunofluorescence analyses in normal human skin and melanomas and analyzed the data. E.A.R. conducted cellular assays. M.D. conducted experimental work. S.V. determined the p53 status of melanoma cell lines and primary tumors. A.Z. did the chromatin immunoprecipitation experiments and analyzed the data. S.H. contributed to the development of MDM4 immunohistochemistry. J.d.L. generated MDM4 knockdown lentiviral vectors. D.Y. and J.G. obtained primary human melanoma samples. J.J.H. contributed to the mouse work and experimental design. H.S. and G.M. generated and characterized BRAF inhibitor–resistant cell lines. F.B. produced and supplied SAH-p53-8 and SAH-p53-8_{F19A}. Y.H., L.L., A.J., R.S.L., G.G., M.S. and F.B. discussed the hypothesis and contributed to data interpretation and experimental design. J.-C.M. conceived the hypothesis, led the project, interpreted the data and wrote the manuscript.

COMPETING FINANCIAL INTERESTS

The authors declare no competing financial interests.

Published online at http://www.nature.com/doifinder/10.1038/nm.2863.
Reprints and permissions information is available online at http://www.nature.com/reprints/index.html.

1. Chin, L., Garraway, L.A. & Fisher, D.E. Malignant melanoma: genetics and therapeutics in the genomic era. *Genes Dev.* **20**, 2149–2182 (2006).
2. Ibrahim, N. & Haluska, F.G. Molecular pathogenesis of cutaneous melanocytic neoplasms. *Annu. Rev. Pathol.* **4**, 551–579 (2009).
3. Cohen, C. *et al.* Mitogen-actived protein kinase activation is an early event in melanoma progression. *Clin. Cancer Res.* **8**, 3728–3733 (2002).
4. Demunter, A., Stas, M., Degreef, H., De Wolf-Peeters, C. & van den Oord, J.J. Analysis of N- and K-ras mutations in the distinctive tumor progression phases of melanoma. *J. Invest. Dermatol.* **117**, 1483–1489 (2001).
5. Papp, T. *et al.* Mutational analysis of the *N-ras*, *p53*, *p16INK4a*, *CDK4*, and *MC1R* genes in human congenital melanocytic naevi. *J. Med. Genet.* **36**, 610–614 (1999).
6. Davies, H. *et al.* Mutations of the *BRAF* gene in human cancer. *Nature* **417**, 949–954 (2002).
7. Gray-Schopfer, V.C., da Rocha Dias, S. & Marais, R. The role of B-RAF in melanoma. *Cancer Metastasis Rev.* **24**, 165–183 (2005).
8. Flaherty, K.T. *et al.* Inhibition of mutated, activated BRAF in metastatic melanoma. *N. Engl. J. Med.* **363**, 809–819 (2010).
9. Chapman, P.B. *et al.* Improved survival with vemurafenib in melanoma with BRAF V600E mutation. *N. Engl. J. Med.* **364**, 2507–2516 (2011).
10. Nazarian, R. *et al.* Melanomas acquire resistance to B-RAF(V600E) inhibition by RTK or N-RAS upregulation. *Nature* **468**, 973–977 (2010).
11. Lane, D.P., Cheok, C.F. & Lain, S. p53-based cancer therapy. *Cold Spring Harb. Perspect. Biol.* **2**, a001222 (2010).
12. Brown, C.J., Lain, S., Verma, C.S., Fersht, A.R. & Lane, D.P. Awakening guardian angels: drugging the p53 pathway. *Nat. Rev. Cancer* **9**, 862–873 (2009).
13. Wade, M. & Wahl, G.M. Targeting Mdm2 and Mdmx in cancer therapy: better living through medicinal chemistry? *Mol. Cancer Res.* **7**, 1–11 (2009).
14. Vousden, K.H. & Prives, C. Blinded by the light: the growing complexity of p53. *Cell* **137**, 413–431 (2009).
15. Chin, L. The genetics of malignant melanoma: lessons from mouse and man. *Nat. Rev. Cancer* **3**, 559–570 (2003).
16. Bardeesy, N. *et al.* Dual inactivation of RB and p53 pathways in RAS-induced melanomas. *Mol. Cell. Biol.* **21**, 2144–2153 (2001).
17. Goel, V.K. *et al.* Melanocytic nevus-like hyperplasia and melanoma in transgenic BRAFV600E mice. *Oncogene* **28**, 2289–2298 (2009).
18. Dovey, M., White, R.M. & Zon, L.I. Oncogenic NRAS cooperates with p53 loss to generate melanoma in zebrafish. *Zebrafish* **6**, 397–404 (2009).
19. Vogelstein, B., Lane, D. & Levine, A.J. Surfing the p53 network. *Nature* **408**, 307–310 (2000).
20. Marine, J.C. & Lozano, G. Mdm2-mediated ubiquitylation: p53 and beyond. *Cell Death Differ.* **17**, 93–102 (2010).
21. Muthusamy, V. *et al.* Amplification of *CDK4* and *MDM2* in malignant melanoma. *Genes Chromosom. Cancer* **45**, 447–454 (2006).
22. Marine, J.C. & Jochemsen, A.G. Mdmx as an essential regulator of p53 activity. *Biochem. Biophys. Res. Commun.* **331**, 750–760 (2005).
23. Toledo, F. & Wahl, G.M. Regulating the p53 pathway: *in vitro* hypotheses, *in vivo* veritas. *Nat. Rev. Cancer* **6**, 909–923 (2006).
24. Danovi, D. *et al.* Amplification of Mdmx (or Mdm4) directly contributes to tumor formation by inhibiting p53 tumor suppressor activity. *Mol. Cell. Biol.* **24**, 5835–5843 (2004).
25. Houben, R. *et al.* High-level expression of wild-type p53 in melanoma cells is frequently associated with inactivity in p53 reporter gene assays. *PLoS ONE* **6**, e22096 (2011).
26. Ackermann, J. *et al.* Metastasizing melanoma formation caused by expression of activated N-RasQ61K on an INK4a-deficient background. *Cancer Res.* **65**, 4005–4011 (2005).
27. Jacks, T. *et al.* Tumor spectrum analysis in p53-mutant mice. *Curr. Biol.* **4**, 1–7 (1994).
28. Jonkers, J. *et al.* Synergistic tumor suppressor activity of BRCA2 and p53 in a conditional mouse model for breast cancer. *Nat. Genet.* **29**, 418–425 (2001).
29. Ferguson, B. *et al.* Differential roles of the pRb and Arf/p53 pathways in murine naevus and melanoma genesis. *Pigment Cell Melanoma Res.* **23**, 771–780 (2010).
30. De Clercq, S. *et al.* Widespread overexpression of epitope-tagged Mdm4 does not accelerate tumor formation *in vivo*. *Mol. Cell. Biol.* **30**, 5394–5405 (2010).
31. Ohsie, S.J., Sarantopoulos, G.P., Cochran, A.J. & Binder, S.W. Immunohistochemical characteristics of melanoma. *J. Cutan. Pathol.* **35**, 433–444 (2008).
32. Bernal, F., Tyler, A.F., Korsmeyer, S.J., Walensky, L.D. & Verdine, G.L. Reactivation of the p53 tumor suppressor pathway by a stapled p53 peptide. *J. Am. Chem. Soc.* **129**, 2456–2457 (2007).
33. Bernal, F. *et al.* A stapled p53 helix overcomes HDMX-mediated suppression of p53. *Cancer Cell* **18**, 411–422 (2010).
34. Vassilev, L.T. *et al.* *In vivo* activation of the p53 pathway by small-molecule antagonists of MDM2. *Science* **303**, 844–848 (2004).
35. Nazarian, R. *et al.* Melanomas acquire resistance to B-RAF(V600E) inhibition by RTK or N-RAS upregulation. *Nature* **468**, 973–977 (2010).

36. Patton, J.T. *et al.* Levels of HdmX expression dictate the sensitivity of normal and transformed cells to Nutlin-3. *Cancer Res.* **66**, 3169–3176 (2006).
37. Wade, M., Wong, E.T., Tang, M., Stommel, J.M. & Wahl, G.M. Hdmx modulates the outcome of p53 activation in human tumor cells. *J. Biol. Chem.* **281**, 33036–33044 (2006).
38. Chapman, P.B. *et al.* Phase III multicenter randomized trial of the Dartmouth regimen versus dacarbazine in patients with metastatic melanoma. *J. Clin. Oncol.* **17**, 2745–2751 (1999).
39. Fedorenko, I.V., Paraiso, K.H. & Smalley, K.S. Acquired and intrinsic BRAF inhibitor resistance in BRAF V600E mutant melanoma. *Biochem. Pharmacol.* **82**, 201–209 (2011).
40. Garcia, D. *et al.* Validation of MdmX as a therapeutic target for reactivating p53 in tumors. *Genes Dev.* **25**, 1746–1757 (2011).
41. Marine, J.C., Dyer, M.A. & Jochemsen, A.G. MDMX: from bench to bedside. *J. Cell Sci.* **120**, 371–378 (2007).
42. Martins, C.P., Brown-Swigart, L. & Evan, G.I. Modeling the therapeutic efficacy of p53 restoration in tumors. *Cell* **127**, 1323–1334 (2006).
43. Ventura, A. *et al.* Restoration of p53 function leads to tumour regression *in vivo*. *Nature* **445**, 661–665 (2007).
44. Xue, W. *et al.* Senescence and tumour clearance is triggered by p53 restoration in murine liver carcinomas. *Nature* **445**, 656–660 (2007).
45. Canner, J.A. *et al.* MI-63: a novel small-molecule inhibitor targets MDM2 and induces apoptosis in embryonal and alveolar rhabdomyosarcoma cells with wild-type p53. *Br. J. Cancer* **101**, 774–781 (2009).
46. Hedström, E., Issaeva, N., Enge, M. & Selivanova, G. Tumor-specific induction of apoptosis by a p53-reactivating compound. *Exp. Cell Res.* **315**, 451–461 (2009).
47. Issaeva, N. *et al.* Small molecule RITA binds to p53, blocks p53-HDM-2 interaction and activates p53 function in tumors. *Nat. Med.* **10**, 1321–1328 (2004).
48. Shangary, S. *et al.* Reactivation of p53 by a specific MDM2 antagonist (MI-43) leads to p21-mediated cell cycle arrest and selective cell death in colon cancer. *Mol. Cancer Ther.* **7**, 1533–1542 (2008).
49. Marine, J.C. MDM2 and MDMX in cancer and development. *Curr. Top. Dev. Biol.* **94**, 45–75 (2011).
50. Flaherty, K.T. Chemotherapy and targeted therapy combinations in advanced melanoma. *Clin. Cancer Res.* **12**, 2366s–2370s (2006).

ONLINE METHODS

Cell culture. MM001, MM011, MM031 and MM117 cells were cultured in F10 medium with 5% FBS (FBS, HyClone) and 5% calf bovine serum (HyClone). A375 and Lu1205 cells were cultured in, respectively, RPMI and DMEM medium with 10% FBS (Sigma). M238, M248, M229 and their BRAF inhibitor resistant sublines were cultured in DMEM plus 5% FBS (HyClone).

Viral transduction. To knock down MDM4 we used two different lentiviral shRNA expression vectors (M:5′-GTGCAGAGGAAAGTTCCAC and M(2): 5′-ACAGTCCTTCAGCTATTT). One of these vectors was described previously[51] and the other was obtained from the Mission shRNA library (Sigma). The p53 knockdown and shRNA control vectors have also been described previously[51].

Cell growth and viability. Cell growth was measured using the WST-1 (Roche) or CellTiter-Glo (Promega) assays. Cells were seeded in triplicate in 96-well plates, and treated with chemotherapeutics: Cisplatin (Sigma) or melphalan (Sigma), SAH-p53-8 and SAH-p53-8_{F19A} (ref. 33), BRAF inhibitor (PLX4032, Selleck Chemicals) or nutlin-3 (Johnson & Johnson) for 24 h. Luminescence was measured in a microplate reader (Victor; PerkinElmer).

Colony-formation assays. Cells were plated at a density between 2×10^3 and 32×10^3 cells per six-well plate and cultured for 12 days. The cells were washed with PBS 1×, fixed and stained 5 min with a 1% crystal violet in 35% methanol solution.

Flow cytometry and apoptosis assays. Cells were incubated for 2 h with BrdU (final concentration 10 μM), washed in PBS and fixed in ice-cold 70% ethanol. Cells were labeled for BrdU incorporation with an APC BrdU flow kit (BD Pharmingen no. 557892), according to the manufacturer's protocol and resuspended in 300 μl of PBS containing 20 μl of 7-AAD. For the annexin V apoptosis assay, melanoma cells were plated at a density of 1.5×10^6 per well in a six-well plate and were treated with SAH-p53-8 or nutlin-3 for 24 h in Opti-MEM. Cells were harvested, washed with PBS, and incubated with Alexa Fluor 488–conjugated annexin V and propidium iodide. Flow cytometry was done in the FACSCanto (BD Biosciences). Apoptosis was also measured using the Caspase-Glo 3/7 assay (Promega).

Western blotting analysis. Cells were lysed in Giordano buffer (50 mM Tris-HCl (pH 7.4); 250 mM NaCl; 0,1% Triton X-100; 5 mM EDTA) containing phosphatase and protease inhibitors (Sigma). 40 μg of each sample was fractionated by SDS-PAGE (Invitrogen; NuPAGE Novex 4–12% Bis-Tris gel) and transferred to a PVDF membrane (iBlot dry blotting system). Membranes were blocked in Tris-buffered saline, 0.2% Tween-20 (TBST) containing 5% or 10% nonfat dry milk, and were subsequently incubated with the appropriate primary antibody. Membranes were subsequently incubated with either horseradish peroxidase–conjugated horse mouse-specific or goat rabbit-specific secondary antibody (Cell Signaling). Proteins were detected by enhanced chemiluminescence (ECL) western blotting detection reagents (Amersham Biosciences) or SuperSignal West Femto maximum sensitivity substrate (Thermo Scientific). The following primary antibodies were used: rabbit MDM4-specific (IHC-00108, Bethyl Laboratories, 1:5000), mouse Mdm2-specific (mixture of a 1:10 dilution of the homemade mouse monoclonal antibodies 2A10 and 4B2 or SMP14, Santa Cruz Biotechnology, sc-965, 1:1000), mouse p53-specific (DO-1, Santa Cruz Biotechnology, sc-126, 1:500), mouse p21-specific (F-5, Santa Cruz Biotechnology, sc-6246, 1:500), mouse β-tubulin–specific (Sigma-Aldrich, T2200, 1:10000), mouse vinculin-specific (Sigma-Aldrich, V9131, 1:10000).

Quantitative real-time PCR. RNA was isolated using the RNeasy minikit (Qiagen) according to the manufacturer's protocol. The RNA was quantified using a NanoDrop 1000 (Thermo Scientific). 2 μg of total RNA was reverse-transcribed using the High-Capacity cDNA reverse transcription kit (Applied Biosystems). Quantitative reverse-transcriptase PCR (RT-qPCR) assays were done using Fast SYBR Green 2× master mix according to the manufacturer's instructions (Applied Biosystems). For normalization, the geometric mean of at least three reference genes was used. For mouse samples, TaqMan probes were designed by Applied Biosystems. For human samples the primers used were as follows: *APAF1* (Fwd, 5′-CCTGTTGTCTCTTCTTCCAGTGT-3′, Rev, 5-AAAACAACTGGCCTCTGTGG-3′), *BAX* (Fwd, 5′-ATGTTTTCTGA CGGCAACTTC-3′, Rev, 5-ATCAGTTCCGGCACCTTG-3′), *MDM4* (Fwd, 5′-AGGTGCGCAAGGTGAAATGT-3′, Rev, 5-CCATATGCTGCTCCTG CTGAT-3′), *MDM2* (Fwd, 5′-AGGAGATTTGTTTGGCGTGC-3′, Rev, 5-TGAGTCCGATGATTCCTGCTG-3′), *BBC3* (Fwd, 5′-GACCTCAAC GCACAGTA-3′, Rev, 5-CTAATTGGGCTCCATCT-3′), *CDKN1A* (Fwd, 5′-AGCAGAGGAAGACCATGTGGA-3′, Rev, 5-AATCTGTCATGCTGGT CTGCC-3′). The following reference genes were used: *GAPDH* (Fwd, 5′-TG CCATGTAGACCCCTTGAAG-3′, Rev, 5-ATGGTACATGACAAGGTGC GG-3′), *HMBS* (Fwd, 5′-GGCAATGCGGCTGCAA-3′, Rev, 5-GGGTACC CACGCGAATCAC-3′), *RPL13a* (Fwd, 5′-CCTGGAGGAGAAGAGGAAA GAGA-3′, Rev, 5-TTGAGGACCTCTGTGTATTTGTCAA-3′), *TBP* (Fwd, 5′-CGGCTGTTTAACTTCGCTTC-3′, Rev, 5′-CACACGCCAAGAAACAG TGA-3′). Gene expression levels and errors in the gene expression levels were calculated using qBasePLUS 1.0 analysis software[52].

Determining BRAF, NRAS and p53 status. 200 ng of cDNA was used as a template for a PCR reaction using the following primers: *BRAF* (Fwd, 5′-AGCACCTACACCTCAGCAGTTACA-3′, Rev, 5′-ACAGGTATCC TCGTCCCACCATAA-3′), *NRAS* (Fwd, 5′-ACAAACTGGTGGTGGTTG GA-3′, Rev, 5′-TGGCCATCCCATACAACCCT-3′). The purified PCR products were sequenced using following nested primers: Primer *BRAF* (Nested) 5′-AGGGCATGGATTACTTACACGCCA-3′, Primer *NRAS* (Nested) 5′-ACTCGCTTAATCTGCTCCCTGT-3′. Genomic DNA was screened for *TP53* mutations at IARC. Exons 2–10 of *TP53* were analyzed by PCR and direct sequencing as described in the protocol available at (http://www-p53.iarc.fr/Download/TP53_DirectSequencing_IARC.pdf). Mutations were screened on both DNA strands and were confirmed in an independent PCR product. The effect of mutations on protein function was determined according to annotations provided in the IARC TP53 database (http://www-p53.iarc.fr)[53].

Histology and IHC. Tissues were fixed overnight in 4% paraformaldehyde, dehydrated, paraffin embedded, sectioned (6 μm) and stained with H&E. For IHC, slides were bleached for 5 h in 10% H_2O_2 solution and stained with antibodies against S-100 (rabbit, Z0311, 1:300; Dako). Detection was done with the secondary goat rabbit-specific antibody (E0432, 1:500; Dako) combined with the incubation in an ABC reagent (Vector). Sections were counterstained with hematoxylin.

Immunofluorescence. Ethics approval was obtained from the Peter MacCallum Cancer Centre Ethics Committee (10/02) for all human tissues and clinicopathological data used in this study. Informed consent was obtained for all human tissues. Formalin-fixed, paraffin-embedded tissue sections used for immunofluorescence analyses were supplied by TissuePath (normal) and the Melbourne Melanoma Project (melanomas). Informed consent was obtained for all human tissues. Tissue sections of 4 μm were dewaxed and antigens were retrieved at 125 °C for 3 min in epitope retrieval solution, pH 9 (Novocastra). For MDM4/Melan A coimmunofluorescence in melanomas, sections were stained on a Dako autostainer. Sections were co-incubated with antibodies against MDM4 (rabbit, IHC-00108, Bethyl Laboratories, 0.5 μg ml^{-1}) and Melan A (mouse, M2-9E3, Santa Cruz Biotechnologies, 2 μg ml^{-1}) for 2 h at room temperature before detection with rabbit-specific and mouse-specific $IgG2_b$ Alexa Fluor secondary antibodies (Molecular Probes; 1:500) for 1 h. Nuclei were counterstained with DAPI (Roche; 20 μg ml^{-1}). MDM4 staining in normal skin was imaged on a Leica SP5 confocal microscope. For image acquisition and analysis of MDM4 expression in melanomas, representative fields were imaged on an Olympus BX-61 microscope at the same exposure and camera settings (including normal skin as control). At least 50 melanoma cells (or normal melanocytes) per sample were individually assessed for mean gray value (MGV) (measure of fluorescence) using ImageJ analysis software by drawing a single line through each cell intercepting the brightest point. MDM4 overexpression was defined as any melanoma sample showing a statistically significantly increase ($P < 0.01$) in MDM4 MGV compared to normal melanocytes, as determined by an unpaired Student's *t*-test (two-tailed).

doi:10.1038/nm.2863

Mice. All animal experiments were carried out in accordance with the guidelines of the University of Leuven Animal Care and Use ethical Committee. All experiments were carried out using pure C57BL/6 males housed in the KU Leuven conventional mouse facility. The subsequent primer sequences were used for genotyping: *Trp53*-null: (Fwd, 5′-ACACACCTGTAGCTCCAGCAC-3′, Rev, (in exon 5) 5′-AGCGTCTCACGACCTCCGTC-3′, Rev, (in the probe) 5′-GTGTTCCGGCTGTCAGCGCA-3′), *Trp53*-floxed (Fwd, 5′-AAGGG GTATGAGGGACAAGG-3′, Rev, 5′-GAAGACAGAAAAGGGGAGGG-3′), *Tyr::NRAS*^{Q61K} (Fwd, 5′-GGCGAAGGCTTCCTCTGTGT-3′, Rev, 5′-GGCC AGTTCGTGGGCTTGT-3′), *Tyr::Cre* (Fwd, 5′-GTCACTCCAGGGGTTGC TGG-3′, Rev, 5′-CCGCCGCATAACCAGTGA-3′. Genotyping of *Mdm4/*^{o} and *Sox2*-Cre mice was done as previously described[30,54].

Xenograft experiments. Eight-week-old Rj:NMRI-nu (nu/nu) female mice were injected subcutaneously with human cell lines in sterile PBS. MM031 xenografts were established by injecting 10^7 cells, whereas Lu1205 and A375 xenografts were established by injecting 10^6 cells. For the knockdown experiments, tumor growth was monitored with a caliper twice a week, and the volume was calculated using the following formula $V = a \times b^2 \times 0.5$, where a is the largest and b the smallest diameter of the tumor. The SAH-p53-8 experiment was done on MM031 cell line–derived tumors with an average volume of 200 mm^3. Cohorts ($n = 7$) were treated with vehicle (5% DMSO in D5W) or SAH-p53-8 (10 mg kg^{-1}), once daily for 5 consecutive d by i.v. injection, and tumor volume was monitored daily for a period of 12 d.

Statistical analyses. Numerical values are reported as means ± s.d. For comparisons between two groups, P values were calculated using either paired or an unpaired two-tailed Student's t tests. For the Kaplan-Meier curves, P values were determined with a log-rank Mantel-Cox test. P values of 0.05 or less were considered statistically significant.

51. Lam, S. *et al.* Role of Mdm4 in drug sensitivity of breast cancer cells. *Oncogene* **29**, 2415–2426 (2010).
52. Vandesompele, J. *et al.* Accurate normalization of real-time quantitative RT-PCR data by geometric averaging of multiple internal control genes. *Genome Biol.* **3**, RESEARCH0034 (2002).
53. Petitjean, A. *et al.* Impact of mutant p53 functional properties on TP53 mutation patterns and tumor phenotype: lessons from recent developments in the IARC TP53 database. *Hum. Mutat.* **28**, 622–629 (2007).
54. Migliorini, D. *et al.* Mdm4 (Mdmx) regulates p53-induced growth arrest and neuronal cell death during early embryonic mouse development. *Mol. Cell. Biol.* **22**, 5527–5538 (2002).